

Flow visualisation of forced flow control over inclined aerofoils

K.L. Powell, K. Parker and J. Soria

Laboratory for Turbulence Research in Aerospace and Combustion (LTRAC)

Mechanical Engineering Monash University

Clayton Campus, Victoria, 3800 AUSTRALIA

ABSTRACT

Dye Flow visualisation experiments are used to investigate the forced flow around a symmetrical aerofoil at various angles of attack. An oscillating cylinder upstream of the aerofoil provides the flow forcing at a Strouhal number of 0.2 and Reynolds number (Re) of 290, based on the cylinder diameter. The effect of the upstream forcing frequency of the flow is achieved by oscillating the upstream cylinder at its natural shedding frequency. This effect is investigated for various spacing (l/d) between the cylinder and aerofoil. Two spacing cases, 2 and 10 diameter are presented here at a pre-stall, stall and post stall angles of attack of 7° , 12° and 17° respectively. These visualisations suggest a degree of control that allows manipulation of the downstream flow structure through an upstream-induced mechanism.

INTRODUCTION

In nature certain species of cetaceans are able to utilise the effect of upstream oscillatory flow conditions to improve their propulsive efficiency. This effect is known as the Katzmayr effect, and was described in 1922 by the Austrian Aerodynamicist Dr Katzmayr. It was noted by [4] that an oscillating wind could reduce the drag on an aerofoil. The Katzmayr effect utilises an upstream oscillating flow condition to reduce aerofoil drag.

It was noted by Tokumaru et al. [5] that a circular cylinder undergoing rotary oscillations about a fixed axis of symmetry can exert a degree of control over the structure of the wake. The wake produced by cylinders in cross flow is known as a von Karman vortex street and is made up of equally spaced vortices of the same strength but alternating in sign. As lift and drag forces are caused by vortex shedding at the surface of the cylinder, the structure of the wake is strongly dependent on the driving frequency of the cylinder. From previous studies it has been found that the frequency of these vortex shedding can be characterised by a dimensionless parameter, the Strouhal number. For a cylinder the Strouhal frequency is approximately 0.21 for any Reynolds number greater than 400. Moretti [3] showed that under forced oscillation two frequencies of vortex shedding exist: one being the same frequency as the unforced cylinder and the other at the forcing frequency.

Experimental studies on cylinders in lock-on synchronisation by Jarza et al. [2] has concluded that oscillations in the incident flow alter the geometry of the vortex street behind an aerofoil. Aerofoils naturally produce lift. Thus the application of the Katzmayr effect on an aerofoil arrangement provides significant potential for application in aerodynamics and hydrodynamics.

Gopalkrishnan et al. [1] experimented with a heaving and pitching NACA0012 aerofoil downstream of a transversely oscillating cylinder. The separation distance between the aerofoil and cylinder was sufficient not to interfere with the vortex formation. In the experiments, the phase between heave and pitch oscillations was varied. The results of these experiments suggested three primary

modes of interaction between the separated flow from the cylinder and the aerofoil.

The work presented in this paper is part of a study to characterise the nature of the interaction between the controlled upstream shedding process on the downstream wake behaviour over an aerofoil. The results presented here describe unique features observed in the tandem arrangement. The effects of an initial angle of attack on a stationary aerofoil, as well as the affect of an aerofoil oscillating at multiples of the Strouhal frequency of the cylinder will be examined, and changes in the cylinder centre to aerofoil leading edge ratio.

The purpose of this investigation is to gain a qualitative understanding through dye flow visualisation, the interactions of periodic disturbances of the incident stream with various parameters as a form of active control for potential thrust optimisation.

EXPERIMENTAL APPARATUS

The experiments were performed in a re-circulating water tunnel at the LTRAC laboratories at Monash University. The tunnel has a five metre long working section, measuring 500mm x 500mm in cross section. The Reynolds number, based on a cylinder diameter of 9.6mm and the steady post acceleration flow velocity of 30mm/s, is equal to 298. Figure 1 shows a schematic drawing of the water tunnel layout.

A cylinder of diameter, $d = 9.6\text{mm}$ was used to form the von Karman vortex street. Downstream a NACA0012 aerofoil with chord, $c = 12\text{mm}$ and $AR = 5.63$, with a maximum thickness, t , equal to the cylinder diameter, $d = t = 9.6\text{mm}$ was used. The aerofoil has an angle of incidence to the freestream of 7 degrees, 12 degrees and 17 degrees. The cylinder contains two dye holes separated by 30 degrees, allowing dye traces in both directions above and below the aerofoil. An optical trigger is used to determine the centre position for both the cylinder and aerofoil. A motion control program was developed to allow controlled, timed shedding of the vortices from the cylinder by oscillating the cylinder at its natural Strouhal frequency. The aerofoil and cylinder are vertically mounted from above the test section. The current experimental setup allows for synchronised oscillations of the downstream aerofoil with the upstream cylinder. The spacing between the aerofoil aerodynamic centre (quarter chord location) and cylinder centre is divided by the cylinder diameter, L/d (spacing/diameter) and is varied to 2, and 10.

The cylinder is oscillated by a stepper motor capable of 80 000 micro-steps per revolution. The stepper motor drivers are controlled by TTL pulses from a Parker AT6400 Indexer. The in-house software allows various oscillation profiles to be achieved by the

cylinder. In the data presented here, the cylinder oscillates sinusoidally accordingly:

$$\theta = \theta_0 \sin(\omega t)$$

where: $\theta_0 = 10^\circ$, ω = frequency of oscillation. Dye is used in order to visualise the behaviour of the flow. The dye is introduced gently into the flow using a needle valve arrangement. Blue and red, are used to highlight the interaction of the upstream disturbance on the wake produced by the aerofoil. Dye flow visualisation is a particle tracing technique, thus the dye follows the path lines in the flow. In an unsteady flow the path lines do not coincide with the instantaneous streamlines and so one must use caution when trying to identify flow features such as vortices. Despite this, dye flow visualisations can provide an idea about the structure of the flow and can be used as a basis to determine areas where more detailed quantitative study can be useful.

The flow is captured on a SONY 120x digital zoom video recorder. In order to adequately capture the field of view the camera is mounted horizontally below the test section. A 45 mirror is used to capture the flow in a wingtip view of the aerofoil and cylinder. In order to identify the phase at which the flow images are captured an optical trigger is used to actuate a LED in the captured video images. Using MGI video wave III, images can be acquired at different phases of the oscillating cylinder from the captured video.

RESULTS AND DISCUSSION

Tests with a circular cylinder in cross flow with forced and unforced oscillation were performed and can be seen in Figures 2 and 3 respectively. It has been shown that oscillating a cylinder at its natural frequency produces controlled timing of the release of vortices behind the cylinder and that two separate frequencies of shedding exist. It can be seen here that the applied forcing on the cylinder appears to form more compact vorticity then compared to the un-forced cylinder, suggesting more intense vorticity that dissipates further downstream due to viscosity when compared to the unforced case. This is in agreement with Moretti [3] who noted that two frequencies of vortex shedding exist at the same time and coexists for a region downstream before other instability affect their superposition and the flow is reorganised into the two vortex patterns. Thus for forcing at the natural Strouhal frequency the superposition of the vortices would suggest more intense vorticity which was observed in the experiments.

In order to compare the effect of the oscillatory flow on the aerofoil, the streamlines of the aerofoil alone was first investigated at a pre-stall, stall and post-stall condition. The stall angle for a NACA 0012 aerofoil is 12 degrees. It was chosen to examine the effect of the stall condition and condition $\pm 5^\circ$. Figure 4 a-c shows the aerofoil at an angle of incidence of 7 degrees, 12 degrees and 17 degrees respectively.

Figure 5, Figure 6 and Figure 7 represents the evolution of a forced oscillatory flow on an aerofoil inclined at seven, twelve and seventeen degrees respectively at 2 diameter spacing at a regular interval through one period of forcing.

The forcing of the cylinder on an aerofoil at 2 diameter spacing causes a stagnation region to exist between the aerofoil and the cylinder. The forcing of the cylinder appears to pulse the stagnation region and shedding can be seen above and below the aerofoil,

although the majority of the dye flow travels above the cylinder. Regions of more intense dye concentration can be seen at periodic spacings downstream along the surface of the aerofoil. The flow appears to stay attached over the entire surface of the aerofoil at all angles of attack, even when the aerofoil is at its characteristic stall angle, twelve degrees. The evolution of the flow as seen in Figure 5-8 is quite similar in structure suggesting repetitious conditions. The mixing of the dyes in the flow visualisation suggest some interaction/mixing between the oscillatory flow and flow from the aerofoil. The flow structure for the forced flow over the aerofoil at the various angles of attack are similar; however the size of the flow structure over the aerofoil increases with increasing angle of attack.

The two-diameter spacing appears to be advantageous in increasing the angle of attack without stall. At this spacing the usual von-Karman vortex street associated with cylinders in cross flow cannot be seen. However, a periodic train of vortices travel down the surface of the aerofoil. The oscillatory flow appear to promote increased mixing down the surface of the aerofoil due to the slower fluid at the boundary layer surface mixing with the free stream velocity, re-energising the boundary layer. In the twelve and seventeen degree angle of attack case the effect of the vortex train acts to promote reattachment of the separated flow by removing the velocity deficit at the boundary layer, delaying stall.

Figure 8, Figure 9 and Figure 10 represents the evolution of a forced oscillatory flow on an aerofoil inclined at seven, twelve and seventeen degrees respectively at 10 diameter spacing at a regular interval through one period of forcing.

The 10 diameter spacing shows various forms of flow that differs from the 2 diameter spacing case. As the angle of incidence increase over this spacing, the wake profile becomes larger. A lower frequency disturbance is notable in the flow at the higher angles of attack (twelve degrees and seventeen degrees) that sinusoidally oscillated the von Karman vortex street. This effect is more prominent as the angle of attack increases and is most likely due to the upstream effect of the stalled aerofoil. Less mixing is evident between the flow from the leading edge and the oncoming vortex street compared with the two diameter spacing case. This flow does not look as favourable as the 2 diameter spacing case and is most likely due to the dissipation of vorticity in the von-Karman vortex street, disabling penetration of the boundary layer.

CONCLUSION

This present experimental study suggests through flow visualisation that it is possible to alter the lift coefficient in pre-stall and post-stall cases via an upstream oscillatory disturbance. The 2 diameter spacing appeared to be the most favourable condition for increase of the stall angle, as the flow still remained attached down a portion of the aerofoil at the 17 degree case. An increase in the spacing revealed that stall occurred earlier than in the 2 diameter spacing case. However, a secondary lower frequency disturbance is evident at the higher angles of attack, twelve and seventeen degrees, which made the flow pattern unsteady with time, producing an oscillating von-Karman vortex street. This effect attached and separated the flow from the surface of the aerofoil at this lower secondary frequency. The von-Karman vortex street oscillated at an angle of ± 30 degrees to the free stream.

REFERENCES

- [1] Gopalkrishnan, R., Triantafyllou, M.S., Triantafyllou, G.S. & Barrett, D., Active vorticity control in a shear flow using a flapping foil., *Jour. Fluid Mech.*, **Vol 7, No. 2**, 1994, 1-21.
- [2] Jarza, A. & Podolski, M., (2004) Turbulence structure in the vortex formation behind a circular cylinder in lock-on conditions, *Euro. Jour. Mech. B/Fluids.*, **Vol 23**, pp.535-550.
- [3] Moretti, P..M., Flow induced vibrations in arrays of cylinder, *Ann. Rev. Fluid Mech.*, **25**, 1993, 99-114.
- [4] Ober, S. (1925) Note on the Katzmayr effect on airfoil Drag, *NACA.*, **No. 214**.
- [5] Tokumaru, P.T. & Dimotakis, P.E., Rotary oscillation control of a cylinder wake, *Jour. Fluid Mech.*, **Vol 224**, pp.77-90.

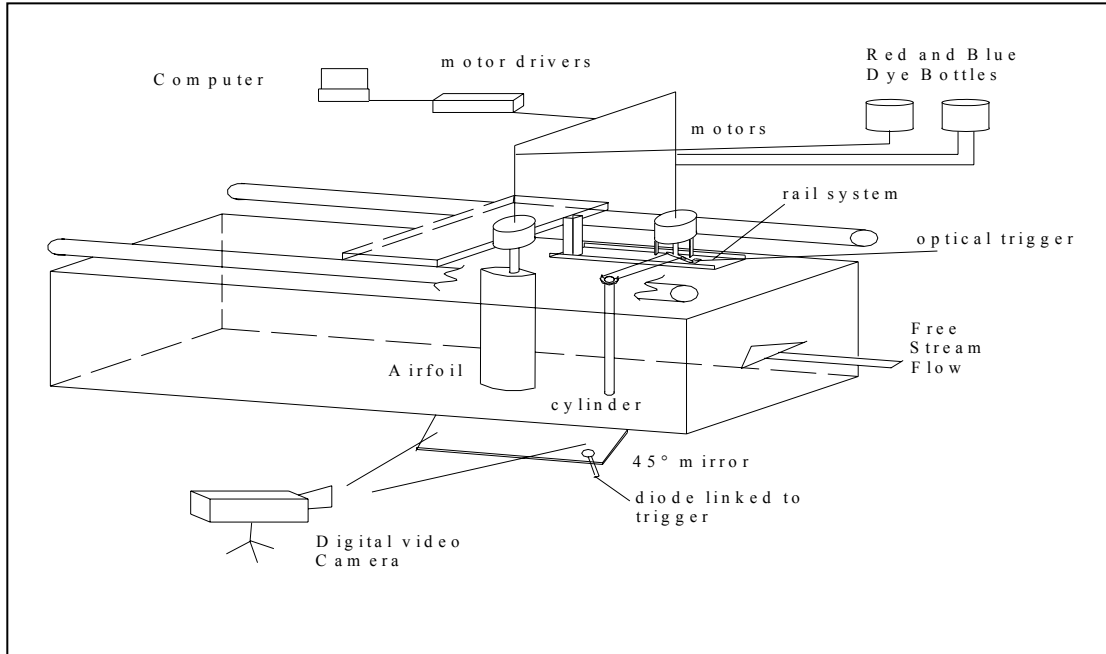


Figure 1: Experimental Setup.



Figure 2: Flow visualisation of the von Karman vortex street produced by forced flow behind a cylinder in cross flow.

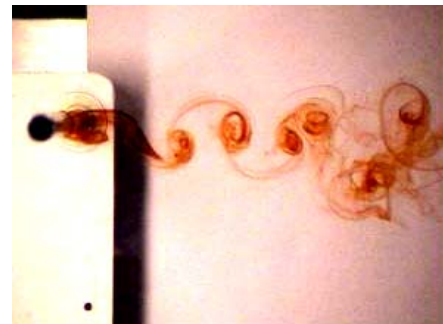
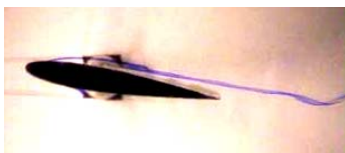
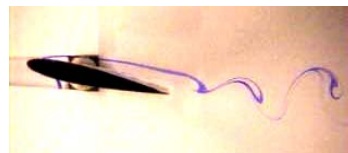


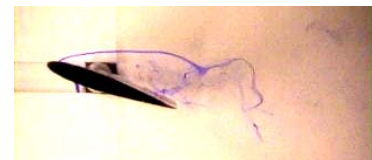
Figure 3: Flow visualisation of the von Karman street formed behind a cylinder in cross flow.



(a)



(b)



(c)

Figure 4 (a-c): Flow visualisation of a NACA0012 aerofoil at 7, 12 and 17 degree angle of attack respectively.



Figure 5: Evolution of the interaction of a forced oscillatory flow with a NACA 0012 aerofoil at a seven degree angle of attack and two-diameter spacing.



Figure 6: Evolution of the interaction of a forced oscillatory flow with a NACA 0012 aerofoil at a twelve degree angle of attack and two-diameter spacing.



Figure 7: Evolution of the interaction of a forced oscillatory flow with a NACA 0012 aerofoil at a seventeen degree angle of attack and two-diameter spacing.



Figure 8: Evolution of the interaction of a forced oscillatory flow with a NACA 0012 aerofoil at a seven degree angle of attack and ten-diameter spacing.



Figure 9: Evolution of the interaction of a forced oscillatory flow with a NACA 0012 aerofoil at a twelve degree angle of attack and ten-diameter spacing.



Figure 10: Evolution of the interaction of a forced oscillatory flow with a NACA 0012 aerofoil at a seventeen degree angle of attack and ten-diameter spacing.